Assessment of Current and Future Climate Change Impact on Soil Loss Rate of Agewmariam Watershed, Northern Ethiopia

Authors: Girmay, Gebrehana, Moges, Awdenegest, and Muluneh, Alemayehu

Source: Air, Soil and Water Research, 14(1)

Published By: SAGE Publishing

URL: https://doi.org/10.1177/1178622121995847

Assessment of Current and Future Climate Change Impact on Soil Loss Rate of Agewmariam Watershed, Northern Ethiopia

Air, Soil and Water Research
Volume 14: 1–11

DOI: 10.1177/1178622121995847

Gebrehana Girmay[1], Awdenegest Moges[2] and Alemayehu Muluneh[2]

[1]Soil and Water Management, Sekota Dryland Agricultural Research Center, Sekota, Ethiopia.
[2]Biosystems Engineering Department, Hawassa University, Hawassa, Ethiopia.

ABSTRACT: Soil erosion is 1 of the most important environmental problems that pose serious challenges to food security and the future development prospects of Ethiopia. Climate change influences soil erosion and is critical for the planning and management of soil and water resources. This study aimed to assess the current and future climate change impact on soil loss rate for the near future (2011-2040), middle future (2041-2070), and far future (2071-2100) periods relative to the reference period (1989-2018) in the Agewmariam watershed, Northern Ethiopia. The 20 models of Coupled Model Intercomparison Project phase 5 global climate models (GCMs) under Representative Concentration Pathway (RCP) 4.5 (intermediate scenario) and 8.5 (high emissions scenario) scenarios were used for climate projection. The statistical bias correction method was used to downscale GCMs. Universal Soil Loss Equation integrated with geographic information system was used to estimate soil loss. The results showed that the current average annual soil loss rate and the annual total soil loss on the study area were found to be 25 t ha^{-1} year^{-1} and 51 403.13 tons, respectively. The soil loss has increased by 3.0%, 4.7%, and 5.2% under RCP 4.5 scenarios and 6.0%, 9.52%, and 14.32% under RCP 8.5 scenarios in the 2020s, 2050s, and 2080s, respectively, from the current soil loss rate. Thus, the soil loss rate is expected to increase on all future periods (the 2020s, 2050s, and 2080s) under both scenarios (RCP 4.5 and RCP 8.5) due to the higher erosive power of the future intense rainfall. Thus, climate change will exacerbate the existing soil erosion problem and would need for vigorous new conservation policies and investments to mitigate the negative impacts of climate change on soil loss.

KEYWORDS: Climate change, RCP scenarios, soil loss, USLE

RECEIVED: August 26, 2021. **ACCEPTED:** January 27, 2021.

TYPE: Advances in Flood Risk Assessment and Modeling – Original Research

FUNDING: The author(s) disclosed receipt of the following financial support for the research, authorship, and/or publication of this article: The study received financial support from the Amhara Agricultural Research Institute.

DECLARATION OF CONFLICTING INTERESTS: The author(s) declared no potential conflicts of interest with respect to the research, authorship, and/or publication of this article.

CORRESPONDING AUTHOR: Gebrehana Girmay, Soil and Water Management, Sekota Dryland Agricultural Research Center, P.O.box: 62, Sekota, Ethiopia. Emails: geberhanagirmay@gmail.com; kesaye1980@gmail.com

Introduction

Soil erosion by water is 1 of the most pertinent problems to the environment.[1,2] The removal of soil from the land surface by erosion is far-reaching all-inclusive, and unfavorably influenced by the efficiency of the all-natural ecosystem.[3] In Ethiopia, the average annual soil loss rate ranges from 16 to 300 t ha^{-1} year^{-1}, primarily depending on the types of land use system, the degree of slope gradient, and the intensity of rainfall.[4,5] It is particularly severe in the highlands where the annual soil loss from agricultural land is estimated to have reached 100 to 300 t ha^{-1} year^{-1}.[6,7] According to some estimates, of 60-million hectares of agriculturally productive land, about 27-million hectares are significantly eroded and 2-million hectares of land are irreversibly lost from productive uses.[7] Soil loss from arable land in the highlands accounts for about 45% of the total land of Ethiopia.[7] Annually, Ethiopia losses more than 1.5*10^9 tons of fertile soil by heavy rain and flood with an associated loss of 1.5*10^6 ton crop production.[8]

Climate change can increase soil erosion, crop damage, and waterlogging, which makes the land difficult or impossible to be cultivated.[8] Climate change will lead to a change in the soil erosion rate due to increased erosive power of precipitation and altered biomass cover.[9-11] Many studies examined climate change's impact on soil erosion around the world.[12-14] According to the Intergovernmental Panel on Climate Change Fifth Assessment Report, precipitation and surface temperature have changed altogether and will continue to change during the 21st century.[15] Changes in temperature and precipitation will impact plant biomass production, infiltration rate, soil moisture, land use, and crop management and hence affect runoff and soil erosion.[16] According to Borrelli et al,[17] global water erosion due to climate change could increase by up (+30% to +66%) over the next 50 years. The study (Moges et al[18]) reported that Ethiopia is 1 of the countries highly affected by increased soil erosion due to climate change. Similarly, a recent study by Moges et al[18] reported a 23% projected soil loss increase in 2050 in 1 of the watersheds of the Ethiopian highland. Although many studies are available for soil erosion quantification under the current climate in Ethiopia,[19-25] very few studies are available that projected soil erosion risk under the face of climate change.[18,26] Thus, it is increasingly necessary to assess the soil loss under the climate conditions to quantify the impact and to plan appropriate adaptation and mitigation measures under local and regional scales.

Empirical erosion models have been frequently used.[27] Among those models, the Universal Soil Loss Equation (USLE) has been commonly used to estimate long-term soil erosion rates from hillslopes within large-scale studies.[28] It depends on easily available soil, topographic, and vegetation

data.[20] The understanding of soil erosion plays a basic part in arranging, planning, and implementing appropriate soil and water conservation approach strategies.[8] In the study area, the land administration strategies being practiced do not consider distinctions in degrees of soil erosion, climate, landscape, soils, and land use and land cover factors. Direct field measurements of soil erosion at permanent research or experimental stations using runoff plots with the known area, topography, and type of soil could give reliable soil loss and runoff,[29] for experimental test purposes. However, the experimental test is exorbitant, labor-intensive, and time-consuming.[28] However, it is conceivable to estimate the average soil loss using empirical models that can be used as forecasting tools for inventories, conservation planning, decision-making, and policy development.[30] Wag Himra and north Wollo are 1 of the highly affected areas by soil erosion in Northern Ethiopia.[31] Understanding the complementary component of soil conservation to confront climate change would help to plan and use appropriate preservation practices. Thus, the objectives of this study were (1) to estimate the current soil erosion using USLE, (2) to predict the rainfall erosivity factor value during the period of 2020s, 2050s, and 2080s using different climate projections from mean Coupled Model Intercomparison Project phase 5 (CMIP5), and finally, (3) to estimate soil erosion in the period of 2020s, 2050s, and 2080s with the corresponding projected rainfall erosivity of the study area.

Materials and Methods

Study area description

The study was conducted at the Agewmariam watershed situated in the Wag Himra Administration zone in Amhara Regional State, Northern Ethiopia. The study area is located at 38° 55' 10" to 38° 56' 10" E longitudes to 12° 31' 40" to 12° 32'30" N latitudes (Figure 1). The elevation of the watershed ranges from 2075 to 2393 m above the sea level. The study area is characterized by a unimodal rainfall pattern; the main rain extends from late June to early September. The mean annual rainfall of the area varied from 689.3 to 1087.9 mm, and the mean minimum and maximum annual temperatures are 12.8°C and 28°C, respectively. The climate of the study area is dry semi-arid lowland.[32] The dominant soil types are eutric cambisols (64.8%) and eutric regosols (35.2%).[33] The landholding size in the watershed is characterized by a small and fragmented plot with less than 0.75 ha per household.[34] The major crops grown are sorghum (*Sorghum bicolor L.*), wheat (*Triticum aestivum L.*), barley (*Hordeum vulgare L.*), teff (*Eragrostis tef [Zucc.] Trotter*), chickpea *(Cicer arietinum L.*), and faba bean (*Vicia faba L.*). The dominant vegetation species are *Acacia etbaica, Acacia tortilis, Acacia seyal, Albizia amara, Olea europaea*, and *Cordia africana*. According to the Bureau of Agriculture, the numbers of heads of the households and the total population in the study area were 259 and 1113, respectively.

Data sources and methods

Soil loss modeling. The USLE[28] was used for soil loss modeling. The soil loss was calculated based on grid cell analyses by multiplying the respective USLE factor values (*R, K, LS, C*, and *P*) using the following equation

$$A = R * K * LS * C * P \tag{1}$$

where A is the annual soil loss ($t\,ha^{-1}\,year^{-1}$), R is the rainfall erosivity factor ($MJ\,mm\,h^{-1}\,ha^{-1}\,year^{-1}$), K is the soil erodibility factor ($Mg\,ha^{-1}\,MJ^{-1}\,mm^{-1}$), LS is the slope length factor (dimensionless), C is the management factor (dimensionless), and P is the conservation practice factor (dimensionless).

Data sources and analysis

Erosivity (R) factors. The R factor was calculated using the equation given by Hurni[35] adapted for the Ethiopian condition which has been derived from spatial regression analysis[36] using equation (2).

The R factor is given by a regression equation as Hurni[35]

$$R = -8.12 + 0.562P \tag{2}$$

where R is the erosivity factor and P is the mean annual rainfall ($mm\,year^{-1}$). The source of precipitation data for the current and future climate is described in climate modeling below.

Soil erodibility (K) factor. Soil samples were collected from the study watershed by a grid of 100 × 100 m, and the sample for analysis was taken from the center of each grid. The 155 soil samples were collected to estimate the physical and chemical properties of the soil. The analyzed soil properties are organic matter content, soil texture, soil structure, and soil permeability. The soil sample analyses were performed based on standard laboratory procedures. Particle size distribution was analyzed using the hydrometer method,[37] whereas organic matter was analyzed by the wet combustion method of Walkley and Black as outlined by Nelson and Sommers.[38]

Soil structure was identified under field conditions with the help of a soil structure assessment kit to determine soil structural class code, shape, and size as adopted from the USLE nomograph.[28] The permeability class code was obtained from soil textural classes,[39] which are encoded from the textural triangle based on the observed soil texture.

Finally, the K factor was calculated from estimated soil properties, namely texture, organic matter, structure, and permeability.[40,41] Using the following equation (equation (3))

$$\begin{aligned} K(\text{factor}) = {} & 2.77 * 10^{-7}(12 - OM)M^{1.14} \\ & + 4.28 * 10^{-3}(s - 2) + 3.29 * 10^{-3}(p - 3) \end{aligned} \tag{3}$$

$$M = \left[(100 - C)(L + Armf)\right] \tag{4}$$

where C is % of clay (<0.002 mm), L is % of silt (0.002-0.05 mm), $Armf$ is % of very fine sand (0.05-0.1 mm), OM is

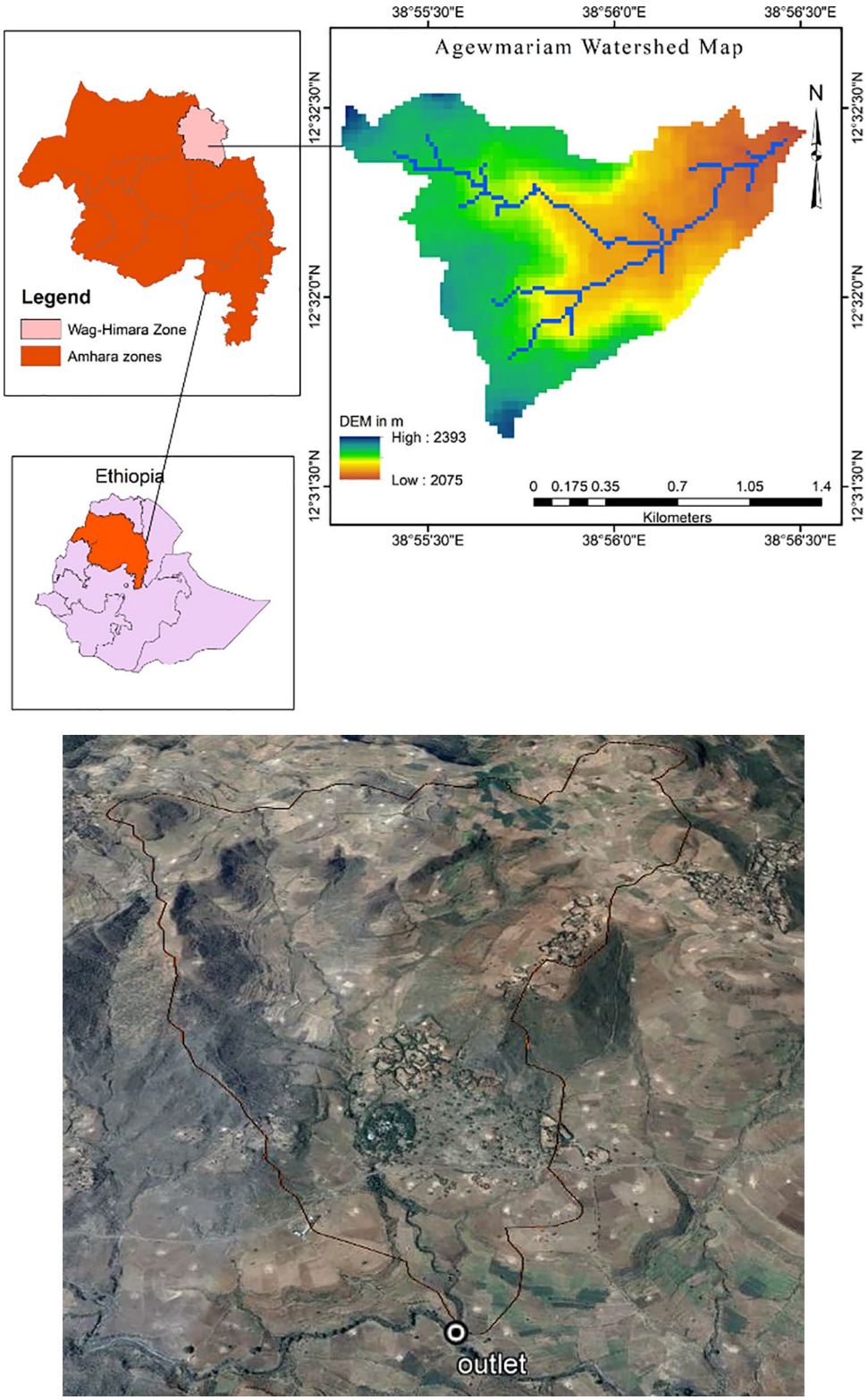

Figure 1. Location map of the study area.

the organic matter content (%), *p* is a code indicating the class of permeability, and *s* is a code for structure size.

Soil sample points of erodibility factors were converted to surface data by interpolation techniques using ordinary kriging in the ArcGIS10.3.1 environment and the Gaussian model.[42]

Slope length and gradient (LS) factor. Slope length and gradient factors were analyzed using a Shuttle Radar Topography Mission digital elevation model with a resolution of 30 m × 30 m by ArcGIS 10.3.1. which is available by the United States Geological Survey (USGS) Earth explorer. The flow accumulation, slope steepness, and slope gradient were estimated. The

LS map was generated using equation (5) developed by Wischmeier and Smith[28] following similar approaches conducted by other researchers[22,25,43]

$$LS = \left(X / 22.1\right)\ m\left(0.065 + 0.045\ S + 0.0065\ S^2\right) \quad (5)$$

$$X = \left(\text{Flow accumulation} * \text{Cell value}\right)$$

where *LS* is the slope length and steepness factor and *X* is the slope length (m). The cell value is 30 m, *m* is a variable slope length exponent, and *S* is a slope gradient (%).

Crop management (C) factor. The *C* factor is the ratio of soil loss from land with specific vegetation to the corresponding soil loss from fallow with the same rainfall.[28] The LANDSAT satellite image from USGS on January 20, 2018, was used to drive land use and land cover map. A supervised classification technique was employed using ArcGIS 10.3.1 software. Land use classification was conducted by the maximum likelihood classification method creating 150 training signatures. A total of 123 reference points were generated from Google Earth for validation. A systematic sampling technique was used to evaluate the accuracy of the land use land cover (LULC) classification of the study area. To measure agreement between image classification, results and ground truth were used based on the user accuracy, producer accuracy, overall accuracy, and kappa coefficient.[44,45] The accuracy assessment was done to check the compatibility of produced classification which exists in reality. The accuracy assessment of the study shows that overall accuracy and kappa coefficient results in the study area were 86.54 and 0.78, respectively, which is beyond a threshold value of overall accuracy mentioned by Hardy and Anderson,[46] while the acceptable level of overall accuracy is above 85%. The kappa coefficient agrees with other similar studies.[44] Finally, 3 land use and land cover types were identified as cultivated, shrubland, and forest. The corresponding *C* values were assigned to each land use and land cover classes using reclassify tools in ArcGIS 10.3.1 environment. Finally, the *C* factor raster layer of the study area was created by assigning the adapted *C* values for each land use and land cover class.

Erosion control practice (P) factor. P factor is the ratio between the soil losses anticipated for a certain soil conservation practice to that of up and downslope plowing.[28] Thus, the *P* factor value data for the USLE model can be collected from field observations.[21,23,25] However, in the study area, there were no soil and water conservation structures. In this condition, the *P* factor for this study was determined using the slope of cultivated land and land use and land cover data as suggested by Wischmeier and Smith.[28] Thus, the *P* values range from 0 to .33 depending on the slope classes of agricultural lands and .8 to 1 regardless of their slope for shrub and forest (Table 2).

Climate change modeling

Both the baseline and future climate data were used in this study. The baseline daily rainfall data were acquired from Koziba weather station (38° 55' 19" E, 12° 29' 3" N) and the Ethiopia Meteorological Agency for the period 1989 to 2018. The projected daily and monthly precipitation data were downloaded from CMIP5 of the Royal Netherlands Meteorological Institute (KNMI) Climate Explorer between 2011 and 2100 under 2 Representative Concentration Pathways, RCP 4.5 (medium stabilization scenario) and RCP 8.5 (high baseline emission scenario). A detailed description of RCP can be found in Van Vuuren et al.[47] The data of 20 models (ACCESS1-0, bcc-csm1-1, BNU-ESM, CanESM2, CCSM4, CESM1-BGC, CSIRO-Mk3-6-0, GFDL-ESM2G, GFDL-ESM2M, HadGEM2-CC, HadGEM2-ES, inmcm4, IPSL-CM5A-LR, IPSL-CM5A-MR, MIROC5, MIROC-ESM, MPI-ESM-LR, MPI-ESM-MR, MRI-CGCM3, and NorESM1-M) from the CMIP5 ensemble and embedded in "Monthly CMIP5 scenario runs" were provided by KNMI Climate Explorer's online File Depot. The RCP 4.5 and 8.5 scenarios were generated under the time scales of the near future (2011-2040), middle future (2041-2070), and far future (2071-2100). Hence, the future climate scenarios were simulated based on the observed climate scenarios.

A statistical bias correction method

Climate model output data are regularly given biased compared with observed time series, and they are making correction procedures necessary.[48] Bias correction methods are correct for the current climate conditions and also valid for future conditions. There are several methods of statistical bias correction analyzing ways.[49] Among the statically bias correction method the delta change approach was used in this study area. The future period of the study area was in 2011 to 2040, 2041 to 2070, and 2071 to 2100 simulated to the baseline period from 1989 to 2018. Future climate time series were constructed using the delta change approach. This involves observed climate time series by mean changes (differences or ratios of changes) simulated with global climate models (GCMs). The changes were determined as monthly precipitation changes (in %) values from the base period during 1989 to 2018. The formula of the delta change bias correction method is as follows[49]

$$P\text{contr}\left(d\right) = P\text{obs}\left(d\right) \quad (6)$$

$$P'_{\text{scen}(d)=}P_{\text{scen}(d)^*}\frac{\mu\text{m}\left(P_{\text{obs}(d)}\right)}{\mu\text{m}\left(P\text{cont}\left(d\right)\right)} \quad (7)$$

P is the precipitation in mm, μ is the mean, *M* is a month, cont is the simulate baseline period, obs is the observed and scen is the simulated scenario future period RCP 4.5 and 8.5.

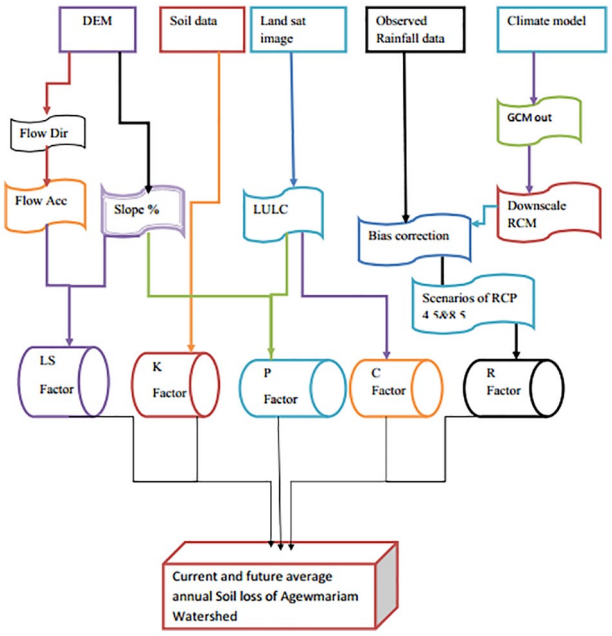

Figure 2. Flowchart of current and future climate change impact on soil erosion. DEM indicates digital elevation model; GCM, global climate model; LULC, land use land cover; RCM, regional climate model; RCP, Representative Concentration Pathways.

Statistical techniques and model performance assessment

Descriptive statistics such as standard deviation, coefficient variance, and relative error were analyzed using IBM SPSS software version 20. The performance of model fit related to precipitation projection and observed data were assessed based on the coefficient of determination (R^2), root mean square error (RMSE), and Nash-Sutcliffe efficiency (NSE). Statistical bias correction was employed to prevent overfitting and underfitting of the data. The future period of 2020s, 2050s, and 2080s was simulated from the CMIP5 scenarios of RCP 4.5 and RCP 8.5 to produce the future estimate of the erosivity factors. Finally, estimates of the future period's soil loss were derived using predicted erosivity factors and the other erosion factors which were affected indirectly by climate change in the study area. Figure 2 shows the detailed process of the methodology.

Results and Discussion

The current rate of soil loss by water

The annual precipitation of the study area was 890.23 mm. The result showed that the average erosivity (*R*) factor value in the study area was 499.2 MJ mm ha^{-1} h^{-1} year^{-1}.

Soil erodibility (*K*) factor in the central and eastern parts of the watershed ranged from 0.079 to 0.129 Mg h MJ^{-1} mm^{-1} and in northern and southern parts of the watershed, it ranged from 0.13 to 0.173 Mg h MJ^{-1} mm^{-1}, which is shown in Figure 3B. The *K* value of the study area ranged from 0.079 to 0.173. The current result also agrees with similar findings reports in the *K* values of tropical soils that range from 0.06 to 0.48,[50] and most Ethiopian soils have the *K* values ranged from 0.05 to 0.6.[51] In contrary to our result, values ranging from 0.018 to 0.033 from Gumra-Maksegnit watershed in the northwestern Amhara[42] and values ranging from 0.0008 to 0.0073 in western Iran[52] were reported. These lower values may be recorded because of high organic matter and surface aggregates. In our study, the mean organic matter was 1.3% in a range from 0.86% to 2.59%, which low organic matter.[53] The high *K* value indicates high erodible and vulnerability to soil erosion which could be attributed to low clay and organic matter contents as less aggregation of soil colloids.[54]

The slope length and gradient (*LS*) factor values ranged from 0 to 311 as illustrated in Figure 3A. The average topographic factor value of the study watershed was 16.33 with a standard division of 26.7. The result showed that the northern and southern parts of the study area, the hillsides, and along the gullies had higher *LS* values. It represents higher susceptibility to erosion; perhaps there will be a greater accumulation of runoff and high velocity.[22,23,25,28,55]

The crop management (*C*) factor for different land uses was derived from satellite images based on land use and land cover maps and its attribute data analysis. The average *C* value in the Agewmariam watershed was 0.053. The cultivated land had a maximum cover factor which could indicate higher erosion. It covers the largest part of the study area indicated in Table 1 and Figure 3C.

Erosion control practice (*P*) factor values were assigned 0.8 and 1, regardless of their slope for shrub and forest. However, *P* value for agricultural land was given accounting for its slope. Hence, the agricultural land is additionally subdivided into 6 classes based on the slope percentage. Different *P* values were assigned for each slope class (0%-5%, 5%-10%, 10%-20%, 20%-30%, and >50%) as illustrated in Table 2 and Figure 3D. High *P* values are obtained from agricultural land on slope classes greater than 30%.

The average annual soil loss was 25 t ha^{-1} year^{-1}, but the soil loss varies from 0 t ha^{-1} year^{-1} in the plain area to 897 t ha^{-1} year^{-1} in the hilly landscapes of the study area. The maximum soil loss happens on the hilly terrains and the mainstream because of the high length and steepness factor value (50-311) and greater than the 30% slope value.[57] The erosion risk was categorized into 5 classes as shown in Figure 4. Accordingly, 67.2% of the total area has a slight erosion rate of 0 to 11 t ha^{-1} year^{-1} and characterized by low-risk areas. The remaining areas (32.8%) were categorized as follows: moderate erosion risk area 5.4% (11-18 t ha^{-1} year^{-1}), high erosion risk area 5.9% (18-30 t ha^{-1} year^{-1}), very high erosion risk area 3.3% (30-50 t ha^{-1} year^{-1}), and severely affected erosion risk area 18.4% (50-897 t ha^{-1} year^{-1}).

Statistical bias correction of global climate data

The GCM output data underestimate in the summer season (July and August) and overestimate in the winter season.

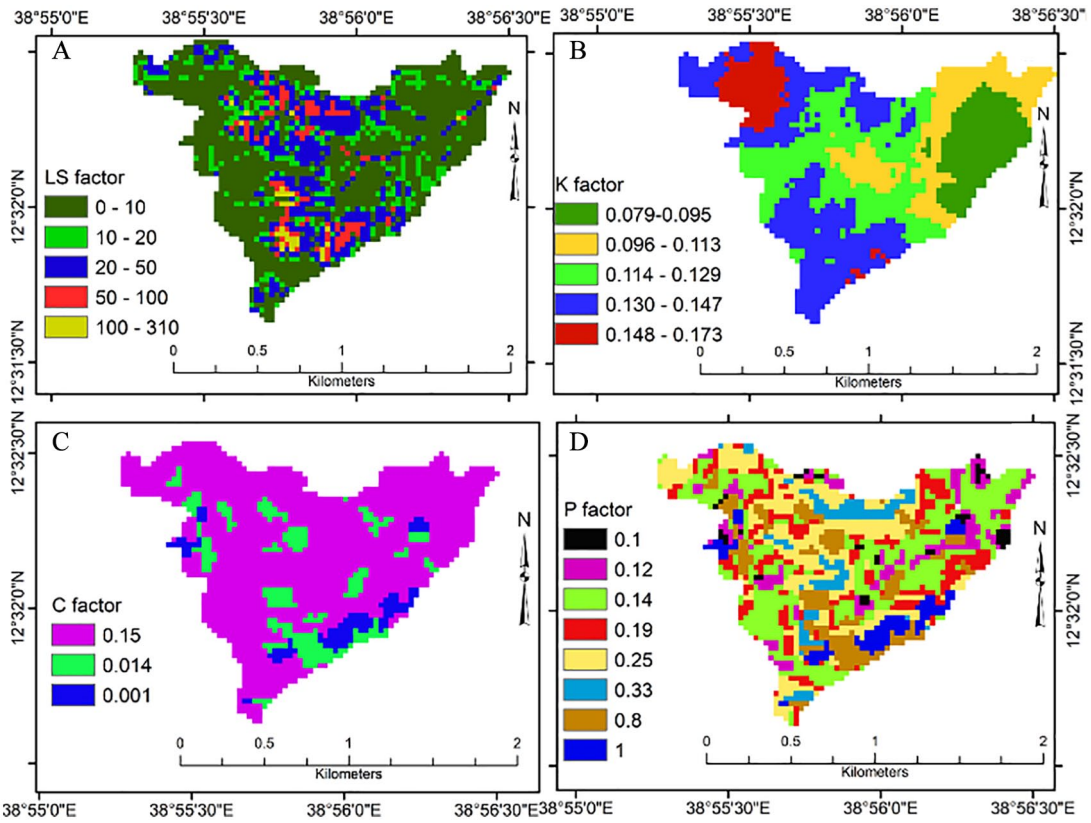

Figure 3. Model parameter map to estimate soil loss in the study area.

Table 1. Land use, area coverage, and cover management factor for the study area.

LAND USE TYPE	AREA IN HA	AREA IN %	*C* FACTOR	REFERENCE
Cultivated land	149.60	81.65	0.15	Hurni,[35] Bewket and Teferi,[21] Amsalu and Mengaw[23]
Forest land	10.55	5.80	0.01	Hurni,[35] Morgan[56]
Shrub land	23.0	12.55	0.014	Wischmeier and Smith,[28] Shiferaw[22]
Total	183.15	100		

Table 2. Conservation practice (*P*) factor values.

LAND USE TYPE	SLOPE CLASS	*P* FACTOR
Agriculture land	0-5	0.10
	5-10	0.12
	10-20	0.14
	20-30	0.19
	30-50	0.25
	>50	0.33
Shrubland		0.8
Forest land		1.00

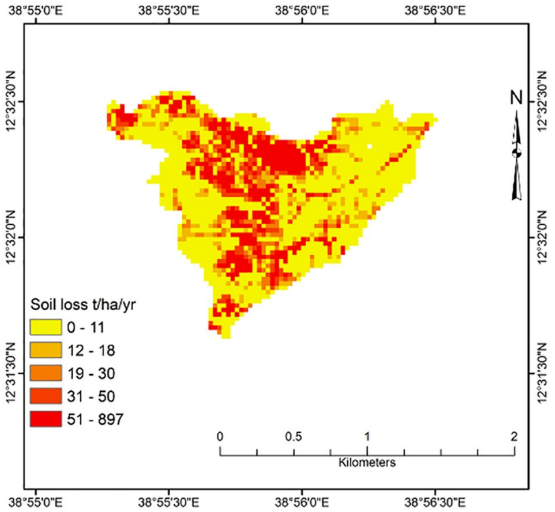

Figure 4. The current (1989-2018) annual soil loss of Agewmariam watershed.

The corresponding model RCP and simulated RCP scenarios from observed mean monthly precipitation were analyzed as indicated in Table 3. The coefficient of determination

(R^2), NSE, RMSE, and percent bias (PBAIS) of the precipitation data are shown in Table 3. The result shows that close up an agreement to the observed value illustrated in Table 3.

The efficiency of predicted precipitation from the climate model was evaluated based on the different model efficiency criteria. The coefficient of determination (R^2) value for raw data of the model and simulated or corrected data of model comparison to observed precipitation data were 0.82 and 0.99, respectively. The result confirms that there was a good relationship performance between the observed and simulated precipitation. The result agrees with the Werri watershed study conducted by Gebremeskel[58] in the Tekeze river basin with an efficiency of 0.92. The statistical tests clearly describe that the raw model has a bias that indicted an overall overestimation of the observed mean monthly precipitation. The bias-corrected value indicated a better fit and shows a positive and small PBIAS value of 0.05, RSME of 1.96, and a strong NSE value of 0.96 as indicated in Table 3. The result agrees with the national-level study conducted by Berhanu et al[59] in whole Ethiopia with the efficiency of RSME (0.87-8.37), NSE (0.95-1), and PBAIS (−1.88 to 2.5).

Future climate scenarios of precipitation and rainfall erosivity

The average annual precipitation was increased by 0.1%, 1.6%, and 1.8% for RCP 4.5 and 2.9%, 5.9%, and 11.8% for RCP 8.5 during the 2020s, 2050s, and 2080s periods, respectively, as indicated in Table 4. Our result concurs with the previous studies conducted at the major Ethiopian river basin including Tekeze,[60] current and future assessments of soil erosion on the Tibetan Plateau in Asia,[14] and Keleta watershed in the Upper Awash basin of Ethiopia[61] using current and future period under both scenarios (Figure 5).

Average annual rainfall erosivity was calculated by using equation (2) for the current period (1989-2018) as well as for the future period (2011-2100) under RCP 4.5 and 8.5 scenarios. Similarly, the average annual erosivity was also calculated for the 3 successive periods, 2011 to 2040, 2041 to 2070, and 2071 to 2100 under both scenarios (Figure 6).

The erosivity value was found to be 492.6, 499.9, and 500.8 MJ mm ha^{-1} h^{-1} year^{-1} for the RCP 4.5 scenario and 506.7, 521.6, and 550.2 MJ mm ha^{-1} h^{-1} year^{-1} for the RCP 8.5 scenario, respectively (Table 4). The rainfall erosivity showed an increasing trend by 0.1%, 1.6%, and 1.8% for the 2020s, 2050s, and 2080s, respectively, under the RCP 4.5 scenario and

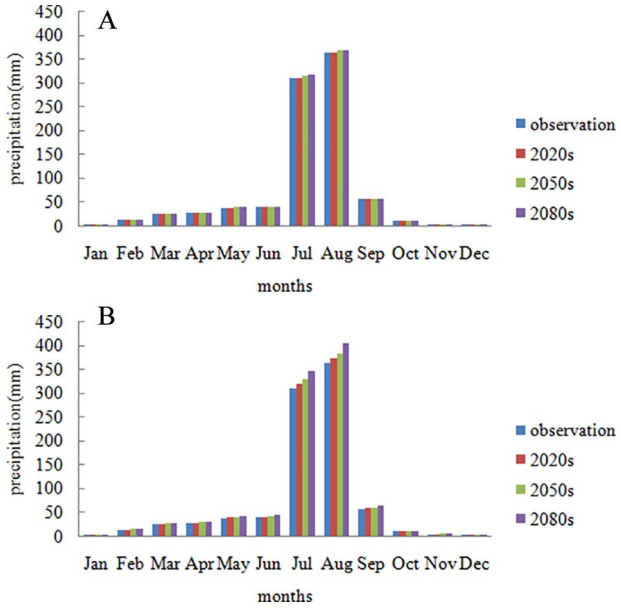

Figure 5. Change in average monthly precipitation for the different future period and scenarios: (A) RCP 4.5 and (B) RCP 8.5 concerning the base period.
RCP indicates Representative Concentration Pathways.

Table 3. Statistical measures of monthly precipitation model output simulated and observed data sets.

	MINIMUM	MAXIMUM	STANDARD ERROR	MEAN	R^2	RMSE	NSE	PBAIS
Observed	3	362	35	74.1				
Simulated RCP	3.1	379	37	77.2	0.99	1.45	0.99	0.05
Model RCP	10.1	193	18	77.1	0.82	14.3	−2	−0.04

Abbreviations: NSE, Nash-Sutcliffe efficiency; PBAIS, percent bias; RCP, Representative Concentration Pathways; RMSE, root mean square error.

Table 4. Change in average annual rainfall erosivity (R) for future period from the base period for RCP 4.5 and RCP 8.5 scenarios.

SCENARIOS	CURRENT	FUTURE PERIOD			RELATIVE CHANGE IN %		
		2020S	2050S	2080S	2020	2050	2080
RCP 4.5	492.19	492.64	499.91	500.85	0.1	1.6	1.8
RCP 8.5	492.19	506.66	521.39	550.2	2.9	5.9	11.8

Abbreviation: RCP, Representative Concentration Pathways.

2.9%, 5.9%, and 11.8% under the RCP 8.5 scenario as illustrated in Table 4.

Projected future soil loss of the study area

The result showed that under the RCP 4.5 scenario, the average annual soil loss increased by 0.76 t ha^{-1} year^{-1} (3.0%), 1.18 t ha^{-1} year^{-1} (4.7%), and 1.29 t ha^{-1} year^{-1} (5.2%) in the period of 2020s, 2050s, and 2080s, respectively, as illustrated in Figure 7B to D and Table 5. Likewise, under the RCP 8.5 scenario, the average annual soil loss increased by 1.5 t ha^{-1} year^{-1} (6.0%), 2.38 t ha^{-1} year^{-1} (9.5%), and 3.58 t ha^{-1} year^{-1} (14.3%) during the period of 2020s, 2050s, and 2080s, respectively, as shown in Figure 8B to D and Table 5 compared with the base period (1989-2018) as indicated in Figures 7A and 8A.

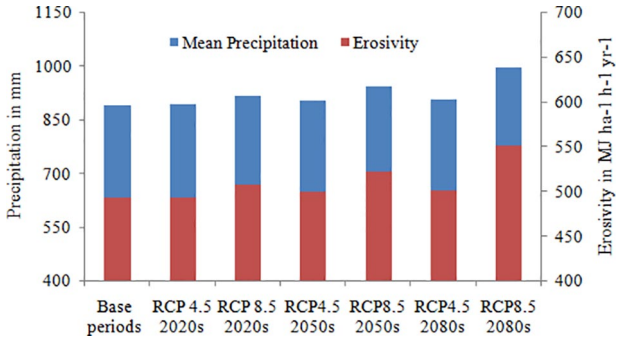

Figure 6. Temporal variation of precipitation and rainfall erosivity in the study area.
RCP indicates Representative Concentration Pathways.

The average annual soil loss rate estimated for the entire watershed was 25 t ha^{-1} year^{-1} which is comparable to other reports by Hurni[35] for the highland of Ethiopia (20 t ha^{-1} year^{-1}); by Ayalew and Selassie[62] for the Guang watershed in the Northwestern Ethiopia (24.95 t ha^{-1} year^{-1}); by Gashaw et al[25] for the Geleda watershed in Northwestern Ethiopia (23.7 t ha^{-1} year^{-1}); and by Amsale and Mengaw[23] for the JabiTehinan watershed in the Northwestern Highlands (30.4 t ha^{-1} year^{-1}). In contrast to our result, some studies reported a high erosion rate in different parts of the Ethiopian highlands. For instance, Bewket and Teferi[21] for the Chemoga watershed of the Blue Nile basin in the Northwestern Highlands of Ethiopia (93 t ha^{-1} year^{-1}) and Gelagay and Minale[24] for the Koga watershed in the Blue Nile basin (47.4 t ha^{-1} year^{-1}). The relatively low average soil erosion rate in our study area could be due to topography with an average slope (27%), and the cultivated areas are located in the gentle slopes of the catchment.

Contrary to our finding, other reported very low average soil erosion rate, for instances, Medago watershed in the Northern Highlands with a rate of 9.63 t ha^{-1} year^{-1} by Brhane and

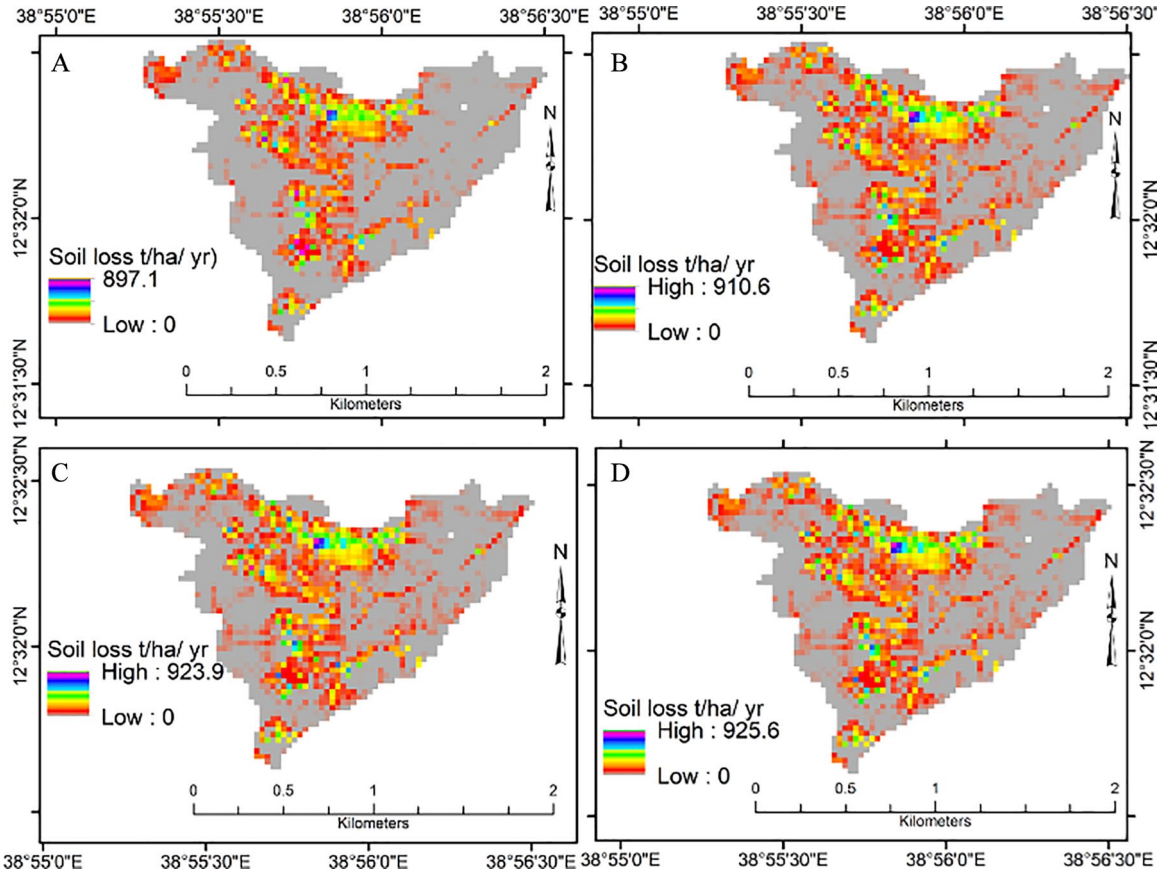

Figure 7. Soil erosion under RCP 4.5 for the (B) 2020s, (C) 2050s, and (D) 2080s periods, respectively, concerning the (A) base period.
RCP indicates Representative Concentration Pathways.

Table 5. Change in soil erosion scenario under RCP 4.5 and 8.5 for the 2020s, 2050s, and 2080s periods, respectively, from the base period.

SCENARIOS	AVERAGE SOIL LOSS (T HA^{-1}YEAR^{-1})				RELATIVE CHANGE (%)		
	CURRENT	2020S	2050S	2080S	2020S	2050S	2080S
RCP 4.5	25.0	25.76	26.18	26.29	3.0	4.7	5.2
RCP 8.5	25.0	26.50	27.38	28.58	6	9.5	14.3

Abbreviation: RCP, Representative Concentration Pathways.

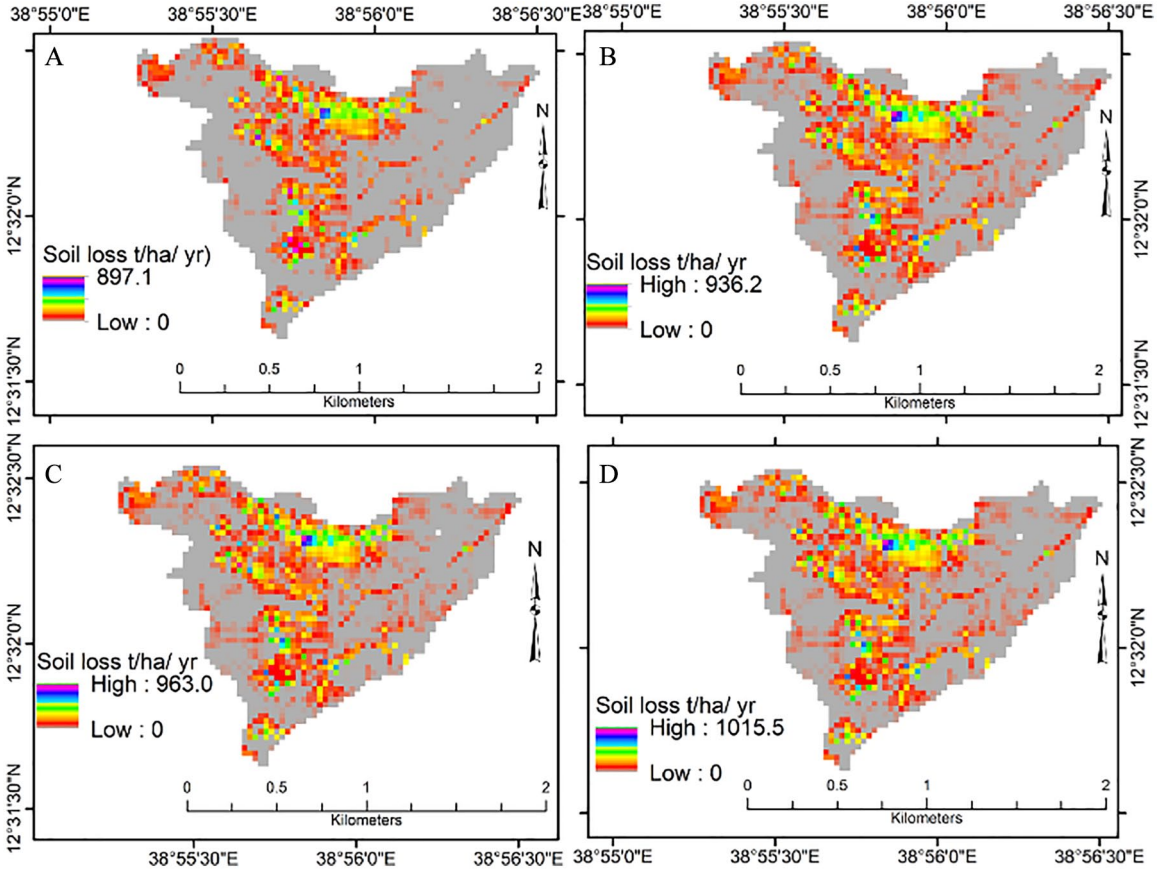

Figure 8. Soil erosion under RCP 8.5 for the (B) 2020s, (C) 2050s, and (D) 2080s periods, respectively, concerning the (A) base period. RCP indicates Representative Concentration Pathways.

Mekonen,[57] 9.1 t ha^{-1} year^{-1} by Gizachew,[63] 7.47 t ha^{-1} year^{-1} by Pongsai et al,[41] 4.17 t ha^{-1} year^{-1} by Eshete,[64] and 4.81 t ha^{-1} year^{-1} by Tiruneh and Ayalew[7] in the highlands of Ethiopia.

These results may be due to the highly variable topographic nature of the Ethiopian highlands, records of the gentle slope feature, and the land use system. In our study area, a high erosion rate was recorded in the steeper slope area of the watershed ranging from 30% to 83% in the steeper slope of cultivated lands which is similar to other studies.[25,57] The results showed a higher mean soil loss rate under RCP 8.5 than RCP 4.5 as illustrated in Table 5, Figures 4 and 5. Our result also confirmed with other reports by Wang et al[65] in the Great Lakes region (4.99%-23.2% increased averagely both scenarios), and Simonneaux et al[13] soil erosion rate increased by 7.9% during the 2080s period in the Rheraya watershed in Morocco.

The rainfall erosivity and soil loss rate were augmented in the period 2020s, 2050s, and 2080s compared with the current period due to high-intensity rainfalls in the study watershed which were also confirmed with other findings.[66-71]

This study results showed the linear relationship between the rainfall erosivity and soil loss under both scenarios and 3 successive future periods. The current findings agree with Lanckriet et al[72] in the May Zeg-zeg catchment in Ethiopia. In contrast to our findings, some studies however reported a decreasing soil loss from the base period. For instance, Zhang et al[68] revealed that the soil loss decreased from the base period by −4% and −6% for the future period of 2016 to 2045 and 2026 to 2035, respectively. This contradictory result may be due to increased rainfall and intensity in our study area. The precipitation and storm intensity changes can be expected to have a greater impact on the soil loss

rate.[10] Accordingly, our results revealed that the future predicted soil loss rate is to increase significantly from the base period for both scenarios due to the higher erosive power of rainfall. The results indicated that the risk of soil loss could be reduced by improving the *C* factor and the degraded land could be recovered by improving the *P* factor. Thus, future soil loss can be mitigated through promoting sustainable land use policy, preventing expansion of other land use types into agricultural land use, and taking soil conservation practices.

Conclusions

This study used the climate model and USLE equation with GIS techniques to assess the current and future impact of climate scenarios on the soil loss rate of Agewmariam watershed. The climate model was evaluated based on the model efficiency criteria. The rainfall is the only changeable parameter that has been considered in this research study, the impact of climate change on soil loss. The increase of rainfall projection in the future with the soil loss. The rainfall erosivity showed an increasing trend by 0.1%, 1.6%, and 1.8% under the RCP 4.5 scenario and 2.9%, 5.9%, and 11.8% under the RCP 8.5 scenario for the 2020s, 2050s, and 2080s, respectively, compared with the base period. This study found out that the total annual soil loss in the study area was 51 403.13 tons moved from the watershed. The average annual soil loss would be increased in the future period compared with the base period. So, climate change scenario prediction studies are providing useful information for decision-makers and local people to plan where and when soil conservation practice should be focused on. A further comparison with climate models and assessment of change in soil loss due to future land use change should be considered for precise estimation of land use dynamic factors.

Acknowledgements

Authors are grateful to the staff of the Sekota Dryland Agricultural Research Center for their frequent technical and logistical support and for creating a good working environment. They are very grateful to the anonymous reviewers for their constructive comments.

Author Contributions

GGi:collected, analyzed, interpreted the data and write up the paper. AMo and AMu: development of the methodology, supervision and review and editing the paper.

REFERENCES

1. Chappell A, Baldock J, Sanderman J. The global significance of omitting soil erosion from soil organic carbon cycling schemes. *Nat Clim Change*. 2016;6:187-191.
2. Teng H, Liang Z, Chen S, et al. Current and future assessments of soil erosion by water on the Tibetan Plateau based on RUSLE and CMIP5 climate models. *Sci Total Environ*. 2018;635:673-686.
3. Pimentel D, Kounang N. Ecology of soil erosion in ecosystems. *Ecosystems*. 1998;1:416-426.
4. Hawando T. *The Survey of the Soil and Water Resources of Ethiopia*. Tokyo, Japan: United Nations University; 1995.
5. Tesfaye A, Negatu W, Brouwer R, Van der Zaag P. Understanding soil conservation decision of farmers in the Gedeb watershed, Ethiopia. *Land Degrad Dev*. 2014;25:71-79.
6. Birhanu A. Environmental degradation and management in Ethiopian highlands: review of lessons learned. *Int J Environ Prot Policy*. 2014;2:24-34.
7. Tiruneh G, Ayalew M. Soil loss estimation using geographic information system in Enfraz watershed for soil conservation planning in highlands of Ethiopia. *Int J Agric Res Innov Technol*. 2015;5:21-30.
8. Tamene L, Vlek PL. Soil erosion studies in northern Ethiopia. In: Braimoh AK, Vlek P, eds. *Land Use and Soil Resources*. Dordrecht, The Netherlands: Springer; 2008:73-100.
9. Nearing MA. Potential changes in rainfall erosivity in the US with climate change during the 21st century. *J Soil Water Conserv*. 2001;56:229-232.
10. Pruski FF, Nearing MA. Climate-induced changes in erosion during the 21st century for eight US locations. *Water Resour Res*. 2002;38:34-31.
11. Pruski FF, Nearing MA. Runoff and soil-loss responses to changes in precipitation: a computer simulation study. *J Soil Water Conserv*. 2002;57:7-16.
12. Gupta S. *Simulating Climate Change Impact on Soil Erosion & Soil Carbon Sequestration* [PhD dissertation]. Bengaluru, India: Indian Space Research Organization; 2015.
13. Simonneaux V, Cheggour A, Deschamps C, Mouillot F, Cerdan O, Le Bissonnais Y. Land use and climate change effects on soil erosion in a semi-arid mountainous watershed (High Atlas, Morocco). *J Arid Environ*. 2015;122:64-75.
14. Misthos LM, Papada L, Panagiotopoulos G, Gakis N, Kaliampakos D. Estimating climate change-based soil loss using erosion models and UAV imagery in the Metsovo Mountain Region. Paper presented at: 4th Joint International Symposium on Deformation Monitoring (JISDM); May 15-17, 2019; Athens, Greece.
15. IPCC. *The Physical Science Basis, the Contribution of Working Group I to Fifth Assessment Reports*. New York, NY: Cambridge University Press; 2013.
16. Li Z, Fang H. Impacts of climate change on water erosion: a review. *Earth-Sci Rev*. 2016;163:94-117.
17. Borrelli P, Robinson DA, Panagos P, et al. Land use and climate change impacts on global soil erosion by water (2015-2070). *P Natl Acad Sci USA*. 2020;117:21994-22001.
18. Moges DM, Kmoch A, Bhat HG, Uuemaa E. Future soil loss in highland Ethiopia under changing climate and land use. *Reg Environ Change*. 2020;20:32.
19. Haregeweyn N, Tsunekawa A, Poesen J, et al. Comprehensive assessment of soil erosion risk for better land use planning in river basins: a case study of the Upper Blue Nile River. *Sci Total Environ*. 2017;574:95-108.
20. Muche H, Temesgen M, Yimer F. Soil loss prediction using USLE and MUSLE under conservation tillage integrated with "fanya juus" in Choke Mountain, Ethiopia. *Int J Agric Sci*. 2013;3:046-052.
21. Bewket W, Teferi E. Assessment of soil erosion hazard and prioritization for treatment at the watershed level: case study in the Chemoga watershed, Blue Nile basin, Ethiopia. *Land Degrad Dev*. 2009;20:609-622.
22. Shiferaw A. Estimating soil loss rates for soil conservation planning in the Borena Woreda of South Wollo Highlands, Ethiopia. *J Sustain Dev Afr*. 2011;13:87-106.
23. Amsalu T, Mengaw A. GIS-based soil loss estimation using RUSLE model: the case of Jabi Tehinan Woreda, ANRS, Ethiopia. *Nat Resour*. 2014;5:49160.
24. Gelagay HS, Minale AS. Soil loss estimation using GIS and remote sensing techniques: a case of Koga watershed, Northwestern Ethiopia. *Int Soil Water Conserv Res*. 2016;4:126-136.
25. Gashaw T, Tulu T, Argaw M. Erosion risk assessment for prioritization of conservation measures in Geleda watershed, Blue Nile basin, Ethiopia. *Environ Syst Res*. 2018;6:1-14.
26. Mengistu D, Bewket W, Lal R. Soil erosion hazard under the current and potential climate change induced loss of soil organic matter in the Upper Blue Nile (Abay) River Basin, Ethiopia. In: Lal R, Singh B, Mwaseba D, Kraybill D, Hansen D, Eik L, eds. *Sustainable Intensification to Advance Food Security and Enhance Climate Resilience in Africa*. Cham, Switzerland: Springer; 2015:137-163.
27. Karydas CG, Panagos P. The G2 erosion model: an algorithm for month-time step assessments. *Environ Res*. 2018;161:256-267.
28. Wischmeier WH, Smith DD. *Predicting Rainfall Erosion Losses: A Guide to Conservation Planning*. Washington, DC: Department of Agriculture, Science, and Education Administration; 1978.
29. Hurni H, Abate S, Bantider A, et al. Land degradation and sustainable land management in the highlands of Ethiopia. In: U. Wiesmann, H. Hurni, eds. *Global Change and Sustainable Development: A Synthesis of Regional Experiences from Research*. Bern, Switzerland: Geographica Bernensia; 2010:187-207.
30. Sadeghi SH, Gholami L, Khaledi Darvishan A, Saeidi P. A review of the application of the MUSLE model worldwide. *Hydrolog Sci J*. 2014;59:365-375.
31. Desta L. *Land Degradation and Strategies for Sustainable Development in the Ethiopian Highlands: Amhara Region*. Nairobi, Kenya: ILRI; 2000.

32. Dejene A. Integrated natural resources management to enhance food security. *The case for community-based approaches in Ethiopia*. http://www.fao.org/tempref/docrep/fao/005/Y4818E/Y4818E00.pdf. Environment and Natural Resources Working Paper No.16. Published July 2003.
33. Jungkunst HF, Krüger JP, Heitkamp F, et al. Accounting more precisely for peat and other soil carbon resources. In: Lal R, Lorenz K, Hüttl R, Schneider B, von Braun J, eds. *Recarbonization of the Biosphere*. Dordrecht, The Netherlands: Springer; 2012:127-157.
34. BOA [Bureau of Agriculture]. *Hag Himra Administration Zone*. Sekota, Ethiopia: Bureau of Agriculture; 2018.
35. Hurni H. Erosion-productivity-conservation systems in Ethiopia. Paper presented at: IV International Conference on Soil Conservation; November 3-9, 1985:654-674; Maracay, Venezuela.
36. Helldén U. *An Assessment of Woody Biomass, Community Forests, Land Use and Soil Erosion in Ethiopia. A Feasibility Study on the Use of Remote Sensing and GIS [Geographical Information System]-Analysis for Planning Purposes in Developing Countries*. Lund, Sweden: Lund University Press; 1987.
37. Gee GW, Bauder JW, Klute A. *Methods of Soil Analysis, Part 1, Physical and Mineralogical Methods*. Madison, WI: Soil Science Society of America, American Society of Agronomy; 1986.
38. Nelson DW, Sommers L. Total carbon, organic carbon, and organic matter. In: Page AL, ed. *Methods of Soil Analysis: Part 2 Chemical and Microbiological Properties*. 2nd ed. Madison, WI: Soil Science Society of America, American Society of Agronomy; 1983:539-579.
39. Boorman DB, Hollis JM, Lilly A. *Hydrology of Soil Types: A Hydrologically-Based Classification of the Soils of United Kingdom*. Wallingford, UK: Institute of Hydrology; 1995.
40. Foster GR, McCool DK, Renard KG, Moldenhauer WC. Conversion of the universal soil loss equation to SI metric units. *J Soil Water Conserv*. 1981;36:355-359.
41. Pongsai S, Schmidt Vogt D, Shrestha RP, Clemente RS, Eiumnoh A. Calibration and validation of the Modified Universal Soil Loss Equation for estimating sediment yield on sloping plots: a case study in Khun Satan catchment of northern Thailand. *Can J Soil Sci*. 2010;90:585-596.
42. Addis HK, Klik A. Predicting the spatial distribution of soil erodibility factor using USLE nomograph in an agricultural watershed, Ethiopia. *Int Soil Water Conserv Res*. 2015;3:282-290.
43. Belayneh G, Moges A. *Erosion Hazard Assessment Using Remote Sensing and GIS: The Case of Gibe-III Dam Catchment, Southwest Ethiopia* [doctoral dissertation]. Dire Dawa, Ethiopia: Haramaya University; 2014.
44. Tilahun A, Teferie B. Accuracy assessment of land use land cover classification using Google Earth. *Am J Environ Prot*. 2015;4:193-198.
45. Vinay M, Mahalingam B. Quantification of soil erosion by water using GIS and remote sensing techniques: a study of Pandavapura Taluk, Mandya District, Karnataka, India. *ARPN J Earth Sci*. 2015;4:103-110.
46. Hardy EE, Anderson JR. A land use classification system for use with remote-sensor data. Paper presented at: LARS Symposia (Paper 2); October 16-18, 1973; West Lafayette, IN.
47. Van Vuuren DP, Edmonds J, Kainuma M, et al. The representative concentration pathways: an overview. *Climatic Change*. 2011;109:5-31.
48. Christensen JH, Boberg F, Christensen OB, Lucas-Picher P. On the need for bias correction of regional climate change projections of temperature and precipitation. *Geophys Res Lett*. 2008;35:L20709.
49. Teutschbein C, Seibert J. Regional climate models for hydrological impact studies at the catchment scale: a review of recent modeling strategies. *Geogr Compass*. 2010;4:834-860.
50. El-Swaify SA. Factors affecting soil erosion hazards and conservation needs for tropical Steeplands. *Soil Technol*. 1997;11:3-16.
51. FAO/UNDP. *The Methodology Used in the Development of Soil Loss Rate Map of the Ethiopian Highlands Field Document 5*. Addis Ababa, Ethiopia: FAO/UNDP; 1984.
52. Vaezi AR, Sadeghi SH, Bahrami HA, Mahdian MH. Modeling the USLE K-factor for calcareous soils in northwestern Iran. *Geomorphology*. 2008;97:414-423.
53. Tadesse T, Haque I, Aduayi EA. *Soil, Plant, Water, Fertilizer, Animal Manure and Compost Analysis Manual*. Addis Ababa, Ethiopia: ILCA; 1991.
54. Bartoli F, Burtin G, Guerif J. Influence of organic matter on aggregation in Oxisols rich in gibbsite or in goethite. II. Clay dispersion, aggregate strength and water-stability. *Geoderma*. 1992;54:259-274.
55. Alexakis DD, Hadjimitsis DG, Agapiou A. Integrated use of remote sensing, GIS and precipitation data for the assessment of soil erosion rate in the catchment area of "Yialias" in Cyprus. *Atmos Res*. 2013;131:108-124.
56. Morgan RP. *Soil Erosion and Conservation*. Hoboken, NJ: John Wiley & Sons; 2009.
57. Brhane G, Mekonen K. Estimating soil loss using Universal Soil Loss Equation (USLE) for soil conservation planning at Medego watershed, Northern Ethiopia. *J Am Sci*. 2009;5:58-69.
58. Gebremeskel G. *Estimation of Groundwater Recharge and Potentials Under Changing Climate in Werii Watershed, Tekeze River Basin* [doctoral dissertation]. Dire Dawa, Ethiopia: Haramaya University; 2015.
59. Berhanu B, Seleshi Y, Demisse SS, Melesse AM. Bias correction and characterization of climate forecast system re-analysis daily precipitation in Ethiopia using fuzzy overlay. *Meteorol Appl*. 2016;23:230-243.
60. Gizaw MS, Biftu GF, Gan TY, Moges SA, Koivusalo H. Potential impact of climate change on streamflow of major Ethiopian rivers. *Climatic Change*. 2017;143:371-383.
61. Bekele M, Daniel A. *Impact of Climate Change, Land Use and Land Cover Changes on the Hydrological Processes of Keleta Watershed, Awash River Basin, Ethiopia* [doctoral dissertation]. Dire Dawa, Ethiopia: Haramaya University; 2017.
62. Ayalew G, Selassie YG. Soil loss estimation for soil conservation planning using geographic information system in Guang watershed, Blue Nile Basin. *J Environ Earth Sci*. 2015;5:126-134.
63. Gizachew A. Geographic information system based soil loss and sediment estimation in Zingin watershed for conservation planning, highlands of Ethiopia. *Int J Sci Technol Soc*. 2015;3:28.
64. Eshete T. *Spatial Analysis of Erosion and Land Degradation Leading to Environmental Stress: The Case of Lake Hawassa Catchement* [doctoral dissertation]. Addis Ababa, Ethiopia: Addis Ababa University; 2009.
65. Wang L, Cherkauer KA, Flanagan DC. Impacts of climate change on soil erosion in the Great Lakes region. *Water*. 2018;10:715.
66. Platts PJ, Poudyal M, McClean CJ. Modelling Shea under climate scenarios. *Report for INNOVKAR Work Package 2*. York, UK: University of York; 2010.
67. Basher LR, Elliott S, Hughes A, et al. *Impacts of Climate Change on Erosion and Erosion Control Methods: A Critical Review*. Wellington, New Zealand: Ministry for Primary Industries; 2012.
68. Zhang Y, Hernandez M, Anson E, et al. Modeling climate change effects on runoff and soil erosion in southeastern Arizona rangelands and implications for mitigation with conservation practices. *J Soil Water Conserv*. 2012;67:390-405.
69. Rao KV, Rejani R, Yogitha P, et al. Estimation of soil loss under changing climatic scenarios in semi-arid watersheds. *Indian J Dryland Agric Res Dev*. 2016;31:89-95.
70. Almagro A, Oliveira PT, Nearing MA, Hagemann S. Projected climate change impacts in rainfall erosivity over Brazil. *Sci Rep*. 2017;7:1-2.
71. Giang PQ, Giang LT, Toshiki K. Spatial and temporal responses of soil erosion to climate change impacts in a transnational watershed in Southeast Asia. *Climate*. 2017;5:22.
72. Lanckriet S, Araya T, Cornelis W, et al. Impact of conservation agriculture on catchment runoff and soil loss under changing climate conditions in May Zegzeg (Ethiopia). *J Hydrol*. 2012;475:336-349.